Evaluation of Outdoor RSS-Based Tracking for WSNs Aiming at Topology Parameter Ranges Selection

Fotis Kerasiotis, Tsenka Stoyanova, George Papadopoulos
Applied Electronics Laboratory, Dept. of ECE, University of Patras, 26504 Rio-Patras, Greece
Industrial Systems Institute, Stadiou Str., 26504 Platani, Patras, Greece
{kerasiotis, tsstoyanova, papadopoulos}@ece.upatras.gr

***Abstract*— The localization and tracking applications are among the most challenging applications, especially when the received signal strength (RSS) is utilized. The RSS is known to be a noisy signal and difficult to use in localization and tracking applications. In the present study we investigate the possibility a target tracking task to be performed with the resources of WSN technology, when using only the RSS of the exchanged messages. We demonstrate that RSS can be used for outdoor localization and tracking application under well-defined topology constraints. The present work presents detailed study about the topology parameter selection when a tracking application is considered. Moreover, the RSS uncertainty is defined in order to be included in the simulation of a tracking scenario. The target tracking considerations by means of tracking techniques, topology parameters and factors influencing the tracking accuracy are combined in simulation examples to evaluate their significance concerning the performance of the tracking task. Furthermore, the propagation model and the topology parameters being identified are used in real outdoor tracking test.**

Keywords – wireless sensor networks, tracking, received signal strength, simulation

I. INTRODUCTION

Wireless sensor network (WSN) is a technology aiming at providing observation of the environmental events and objects with minimal human supervision. The field of WSN encompasses a very broad array of applications including monitoring systems, smart environments, target localization and tracking and a lot of others.

The base of any localization and tracking system is the mechanisms used to determine the position of a fixed or a mobile object by measuring physical distances in indirect way. Different techniques, which provide relation between the distance and some measurable parameter of the transmitted signal, such as time of flight, time difference of arrival, angle of arrival and the strength of the measured signal, can be utilized.

The target tracking applications are based on localization information exchange among the sensor network nodes, which require collaborative sensing, communication and computation among multiple sensors that observe the target objects. The network topology and the influence of the environment on the in-network communication and on the signal used for tracking are also important factors that need consideration [1]. In general, the target tracking application scenario is composed of four functional components, namely deployment, localization, target tracking and information exchange.

Sensor nodes' deployment reflects two main aspects of a WSN, namely sensing and communication. The main sensor network problems that the deployment addresses are related to optimal area coverage and network connectivity [2]. When tracking application is concerned, defining of the deployment constraints and the topology parameters is also part of the deployment phase. After the network topology is formed the localization task begins. Various localization methods, presented in the literature, are generally divided in range measuring algorithms [3-5] and range-free algorithms [6-8]. When the positions of all sensor nodes within the network are determined, the tracking task can be implemented. Since the main goal of tracking is localization of moving objects, some of the above mentioned localization methods, mostly the range measuring algorithms, could be also utilized. Additionally, tracking oriented algorithms and protocols, based on mobile agents and its data fusion or using binary detection have been also developed [9-11].

The RSS-based localization-tracking techniques that deal with position estimation mainly belong to two categories, namely trilateration or multilateration, which depends on the number of used beacon nodes, and fingerprinting. Trilateration uses a signal propagation model to extract the RSS/distance relation, and together with the beacon nodes' position to estimate the position of a mobile object. On the other hand, the fingerprinting approach is based on acquiring reference points within the target area. To these reference points signature vectors are associated consisting RSS data taken by each of the beacon nodes. The signature vector is formed either by real measurements in the target environment, either by simulation performed with an appropriate for the environment RF propagation model. All reference points' positions and their signatures construct a database. During the localization phase, the RSS measurements, taken from the beacons for a particular mobile object, form a tested signature. The tested signature is compared with the signatures in the database to find the likeliest one and the corresponding reference point location is accepted as a location for the mobile object.

Most of the RSS-based state-of-the-art localization and tracking algorithms for outdoor environment utilize a propagation model to discover the distance, relying on that the RSS decreases with the distance by well-known physical

low. However, most of the proposed tracking algorithms use simplistic models, usually supposing an ideal exponential characteristic of the RSS variation due to distance, without taking into consideration the influence of the environment and the topology parameters to the propagation characteristic [5, 6, 9]. Thus, the present state-of-the-art localization and tracking techniques do not offer satisfying solutions to major localization/tracking problems and applying them successfully in real outdoor tracking applications is doubtful.

In general, many factors have to be considered when a RSS-based tracking application is designed, starting from selection of proper propagation model, which has to represent in a relatively accurate way the interaction between the RF signal and the environment. The topology parameters, such as number of beacons, beacons' height and optimal beacons' distance, have to be also evaluated for their optimal values.

The study in previous work on RSS behavior for varying impact factors [12], has led to important conclusions that drove the research presented in [1] and extended in the present work. In the present study we investigate the possibility a target tracking task to be performed with the resources of WSN technology, when utilizing only the radio signal strength (RSS) of the exchanged messages. RSS is notorious for being a noisy signal that is difficult to use for ranging-based localization and tracking applications. In this study, we demonstrate that RSS can be used for outdoor localization and tracking application under well-defined topology constraints.

The present work elaborates on [1], by means of presenting more detailed study about the topology parameter selection, the RSS uncertainty identification and including it in the simulation of tracking scenario, more simulation examples and finally, performing of real outdoor tracking test. All real measurements were performed with Tmote Sky [14] or TelosB [21] sensor nodes, which both have CC2420 radio chip. Their working frequency is at 2.4GHz band. Taking advantage of the measurements performed for [23] we selected the central frequency of channel 26, i.e., 2.48GHz, as working frequency due to not overlapping with the available in the areas WLANs. All simulations were performed with the selected radio frequency.

The rest of the paper is organized as follows: In Section II, the most important problems encountered in a tracking application are presented, including the influence of the RF propagation, the deployment constrains and the topology parameters on the tracking performance. Section III discusses the influence of the mobile node position on the RF signal propagation in order to identify the most promising ones. The target tracking considerations by means of tracking techniques, topology parameters and factors influencing the tracking accuracy are presented is Section IV followed by simulation examples. In Section V the propagation characteristics and topology constraints identified in the previous sections are used in real outdoor tracking test. Finally, Section VI concludes this work.

II. ANALYSIS OF TRACKING PROBLEM DIMENSIONS

The tracking application scenario under consideration is based on a triangular topology of fixed nodes and has two main objectives: (1) localization of the triangle, inside which the mobile node moves and (2) tracking the position of the mobile node, which is placed on human body. The tracking application approach is based on the assumption that the mobile node transmits packets periodically and the fixed nodes determine the mobile node's position by measure the RSS of the packets. Such a tracking algorithm has been implemented making use of mobile agents [9].

The tracking application scenario under study is shown in Fig. 1. It concerns outdoors target-tracking, using the widely-used Tmote Sky or TelosB sensor nodes. The fixed sensor nodes, named also beacons, are deployed in triangular grid. The server, which is to be placed probably in a building, receives information from the fixed WSN nodes about the position of the mobile nodes, i.e., the people, as well as additional information such as: patient vital signs. The application under consideration should satisfy specific constraints:

- Accuracy of the tracking process: up to 10m
- Sampling period of the target node location: 1sec
- Topology: fixed nodes in triangular grid at approximately 50m distance.

The study in the present work is focused on the second objective mentioned above, i.e., tracking the position of the mobile node inside the triangle, and more specifically, on identifying the most crucial RSS-based tracking problems, and determining and evaluating the topology parameters that can guarantee successful tracking. Based on this, the aims of the present study can be formulated as follows: (1) evaluation of the behaviour of the propagated RF signal in order to identify the important RSS-based tracking problems, (2) selection of the topology related parameters, when taking into consideration the tracking task requirements and the deployment constraints, (3) use of the selected propagation model and topology parameters to simulate a target tracking task, and (4) keeping the proposed topology parameters to perform real outdoor tracking test.

In the following sections the factors that may cause tracking problems, i.e., impossibility to perform tracking, are discussed.

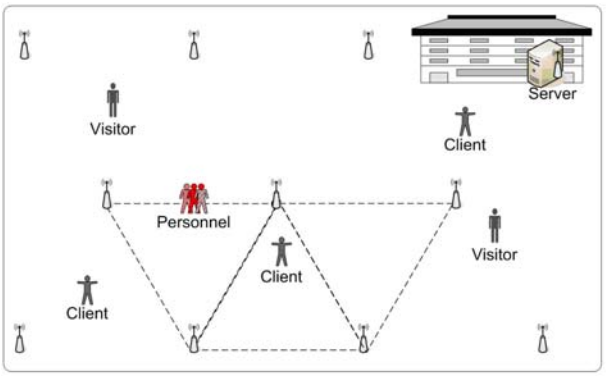

Figure 1. Tracking application scenario

A. *Basic characteristics of the behavior of the propagated signal*

As shown in [12], theoretical models can describe the behaviour of a transmitted signal from the receiver side, considering free space and ground surface reflections. The main parameters affecting the RF signal propagation are the height from the ground for the transmitter-receiver pair (T-R), the frequency of the transmitted signal and the type of the ground (e.g. grass), assuming that the environment is open space without obstacles. In another work [18] we introduced FOM, a model for free space outdoor environments, where the effect of some other important parameters on propagated signal such as variation of transceivers, radio frequency gain, antenna pattern irregularities, and RSS uncertainty, are also considered. Fig. 2 presents real outdoor measured data and simulated data, performed with FOM. For these measurements and simulations the receiver height is at 2m and the transmitter height is at 1.1m in Fig. 2(a) and at 0.08m in Fig. 2(b). The results show a good correspondence between real measurements and simulation. The results presented here as well as those in [18] confirm that this model can be used during the evaluation of the topology parameters with sufficient accuracy of the tracking task for the target application.

The model described in [18], i.e., FOM, is used in the rest of the paper, when a simulation of the RF propagation is mentioned. Its formulation is given with (1) and (2).

$$\overline{P_R}(d) = P_T\left(\frac{\lambda}{4\pi d}\right)^2\left(K_1^2 + K_2^2\Gamma^2 + 2K_2\Gamma\cos\left(\frac{2\pi}{\lambda}\Delta L\right)\right) \quad (1)$$

where $\overline{P_R}(d)$ is average value of the received power.

When P_R is expressed in decibels with RSS uncertainty included as $X_{\sigma(\overline{P_R})}$, then the formulation is:

$$P_R = \overline{P_R}(d) + X_{\sigma(\overline{P_R})} \quad (2)$$

where P_R is the received power, P_T is the transmission power, d is T-R distance, λ is the wavelength, Γ is the ground reflection coefficient, ΔL is path length difference between the direct and the reflected signals, coefficients K_1 and K_2 are antenna specifics representing the gain in particular antenna orientation, which are described in detail in [18]. The RSS uncertainty is given as a Gaussian random variable X with distribution $\sigma(\overline{P_R})$.

Fig. 3 shoes three simulations of the RF propagation, when the fixed node is at 2m, and the mobile node is at 0.1m, 0.5m and 1.4m. One important observation regarding the effect of the ground reflection phenomenon on the RSS is that the reflected and the direct signals interact and create 'nulls', where the RSS is very low and quite variable, as we observed in [12], [18] and [22]. Another observation is that the 'null' areas move with the change of the height, which is connected with the change of the path length of the direct and reflected signal and phase difference.

From the tracking algorithm point of view, one could conceivably take advantage of these 'nulls' and through trilateration, combine the RSS levels of the three fixed nodes to distinguish the possible positions of the mobile node in a triangular region. The pattern effect on the RSS-based tracking scheme of Fig. 3 is investigated in Section III, so as to highlight the risks and uncertainties that it may produce. A more promising approach is to ensure that the RSS characteristic is "smooth", that is to have as few as possible 'nulls'. This can be achieved by judicious selection of the heights at both transmitter and receiver.

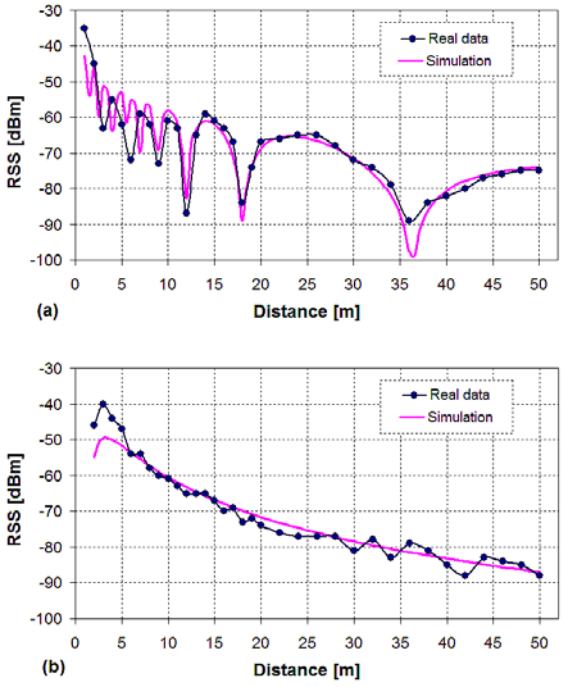

Figure 2. Simulation vs. experimental RSS characteristic for receiver at 2 m and transmitter at: a) 1.1m and b) 0.08m

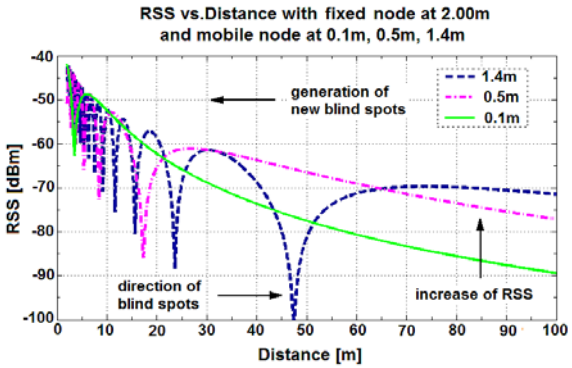

Figure 3. Propagated signal for different mobile node heights and fixed nodes at 2m

B. Deployment constraints

Based on experiments and simulations performed in previous work [22], we discovered that the combination between the fixed node's height and distance is limited, considering the fact that the communication among them has to be as robust as possible with respect to minimum packet loss. This limit, also named safe RSS threshold, is defined by that RSS level, at which the packet loss increases more than 5%, and this is about -80dBm. Therefore, the heights which can be chosen for the fixed nodes are defined according to this RSS level. Fig. 4 shows simulation, where the RSS is simulated with respect to the fixed nodes heights (between 0.10m and 3m) for distance at 50m, which is one of the topology requirements. The red doted horizontal line expresses the safe RSS value, which is the minimum value for reliable communication among the fixed nodes. Therefore, the selected heights of the fixed nodes for reliable communication among them at distance of 50m are: (a) 0.50m–1.65m, (b) 1.85m–2.35m, and (c) 2.55m–2.90m.

C. Mobile node positions on the human body

Having assured a robust communication for the fixed nodes by heights selection as described above, the next parameter under consideration is the height of the mobile node. Possible positions of the mobile node on the human body are: ankle, knee, waist, wrist, chest and arm, shown in Fig. 5. Table I shows the correspondence of each of these positions with the average heights from the ground including also the variation which may be introduced due to movements of the human. There are small height variations for some body parts such as knee and ankle and greater ones for others such as waist, chest and arm and even greater considering the movement of the wrist when raising. These variations are caused by every possible movement the human target can perform, such as walking, running, sitting, bending and raising his/her hands.

TABLE I. MOBILE NODES POSITIONS ON THE HUMAN BODY AND VARIATION DUE TO MOVEMENTS

Position on Human Body	Standing Position Height	Height Variation Including Body Movement
Chest	1.4 m	from 0.9 to 1.45 m
Arm	1.4 m	from 0.9 to 1.45 m
Weist	1.1 m	from 0.5 to 1.20 m
Wrist	1.0 m	from 0.5 to 2.00 m
Knee	0.55 m	from 0.45 to 0.70 m
Ankle	0.15 m	from 0.15 to 0.30 m

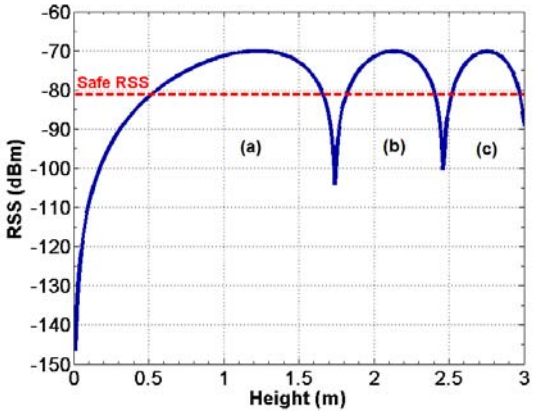

Figure 4. Deployment constraints for the choice of fixed nodes' height

D. RSS-based mobile node position estimation

When the tracking task is performed through beacon nodes, the position estimation of a mobile object can be performed via two techniques: fingerprinting and trilateration. Trilateration uses the signal propagation model and the beacon nodes positions to convert RSS values to a distance measurement so as to estimate the position of a mobile object with trilateration techniques. On the other hand, the fingerprinting approach is based on acquiring reference points within the target area (the triangle in our case). To these reference points are associated signature vectors consisting of RSS data taken by each of the beacon nodes. The signature vector is formed either by real measurements in the target environment, or by simulation performed with an appropriate for the environment RF propagation model. All reference points positions and their signatures construct a database. During the localization phase, the RSS measurements taken from the beacons for a particular mobile object form a tested signature. The tested signature is compared with the signatures in the database to find the likeliest one and then the corresponding reference point location is accepted as a location for the mobile object.

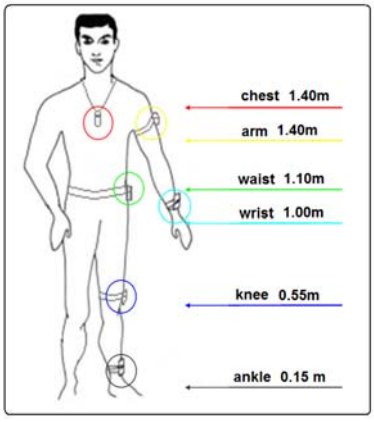

Figure 5. Possible positions of the mobile node on the human body

For the purpose of this work the fingerprinting approach is considered and two techniques for defining the locations of the reference points are evaluated, namely quantized levels and square grid. In the quantized levels, the RSS in the range between -40dBm and -90dBm is divided in discrete levels, to which correspond different distance regions. Using the RF propagation model to simulate the propagation within the triangle, the location of the reference points is chosen so that at least one reference point can exist in each region, differentiated by the discrete levels. The square grid approach for positioning of the reference points is quite simple. The target area is divided out in small squares, the size of which determines the minimum localization accuracy. Detailed analysis of these two techniques is offered in Section IV.

Summarising the issues discussed in this section the following conclusions were derived:

- The RF signal propagation has to be considered while choosing the topology parameters, such as beacons' distance and height, in order to assure reliable communication between the beacons.
- The position of the mobile node on the human body should be selected so as to minimize the node's height variation due to body movement and exclude the 'nulls' from the propagation curve.
- When using fingerprinting approach the selection of the reference points' locations needs preliminary evaluation according to well defined criteria such as: number of reference points, accuracy, simplicity of generation, etc.

III. MOBILE NODE POSITION EVALUATION

In previous work [12, 18], it has been shown that the height of the sensor nodes heavily affects the behavior of the propagated signal. Moreover, the deployment constraints for reliable communication limit the possible fixed nodes' height within the ranges determined in the previous section as 0.50m – 1.65m; 1.85m – 2.35m, and 2.55m – 2.90m, for 50m distance between the beacon nodes. Therefore, in this section, the RSS behaviour is studied with respect to the possible mobile node positions listed in Table I.

A. Analysis of the mobile node at upper heights

Assuming that higher placements are selected for the mobile node on the human body e.g. chest, arm, wrist and waist, we select the height at 1.1m as a representative height for the mobile node. The corresponding behaviour of the propagation signal when the mobile node is at 1.1m is shown in Fig. 6. The simulation is performed through (1) for four fixed nodes' heights selected from the regions suggested by the deployment constraints for fixed nodes, as follows: 0.55m and 1.40m are from region (a), 2.10m is from region (b) and 2.7m is from region (c) in Fig. 4. Analysing the results shown in Fig. 6, it is noticeable that when the mobile node is placed at 1.1m and the fixed nodes' height is 2.10m or 2.70m, the RF propagation between 1m and 50m is full of 'nulls' and to extract distinguishable RSS/distance combinations for the quantizing tracking technique is impossible. The case when the fixed nodes are at 1.40m height presents less 'nulls', but the problem with separating the signal propagation on distinguishable RSS/distance combinations still exists. The last beacons' height of 0.55m is more promising in the sense that the RSS curve is smooth and some distinct regions can be derived for the distances between 15m and 50m. The drawback is that the difference between the RSS in 15m and the RSS in 50m is only 12dBm, which implies separation in no more than two regions. Using only two regions cannot provide acceptable tracking accuracy.

As a conclusion of this analysis, when the mobile node is at about 1.10m height, there is no appropriate height for the beacon nodes so as to guarantee reliable communication between the beacon nodes and consequently successful tracking.

B. Analysis of the mobile node at low heights

According to Fig. 5 and Table I the lower heights for placement of the mobile node on the human body are: the knee at height of 0.55m and the ankle at height of 0.15m. To analyse the behaviour of the propagated RF signal when the mobile node is at 0.55m and 0.15m, simulations are performed. The results for the mobile node height at 0.55m are shown in Fig. 7(a), and for the mobile node height at 0.15m in Fig. 7(b). For both mobile node's heights the fixed nodes are at heights selected from the regions suggested by the deployment constraints for fixed nodes, i.e., 0.55m and 1.60m from region (a); 2.10m from region (b) and 2.7m from region (c) in Fig. 4.

Referring the results in Fig. 7(a) for mobile node at 0.55m, the RF propagation results for the beacons' height at 2.7m, 2.10m and 1.60m show similar problems to those of the waist case. This makes the particular beacon heights inappropriate for a successful tracking task. The smallest beacon height of 0.55m seems more promising for the distances between 6m and 50m. The propagation curve has good slope, which gives variance between the RSS at 6m and the RSS at 50m of about 25dBm. This variance suggests the use of the traditional tracking methods with linear models and filters as well as the quantized levels technique.

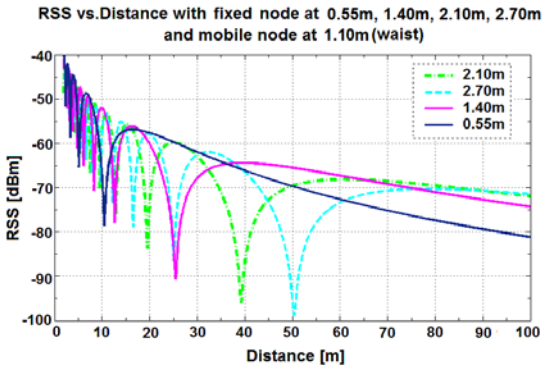

Figure 6. Behavior of the propagated signal or RSS concerning different heights for the fixed nodes and waist mobile node position

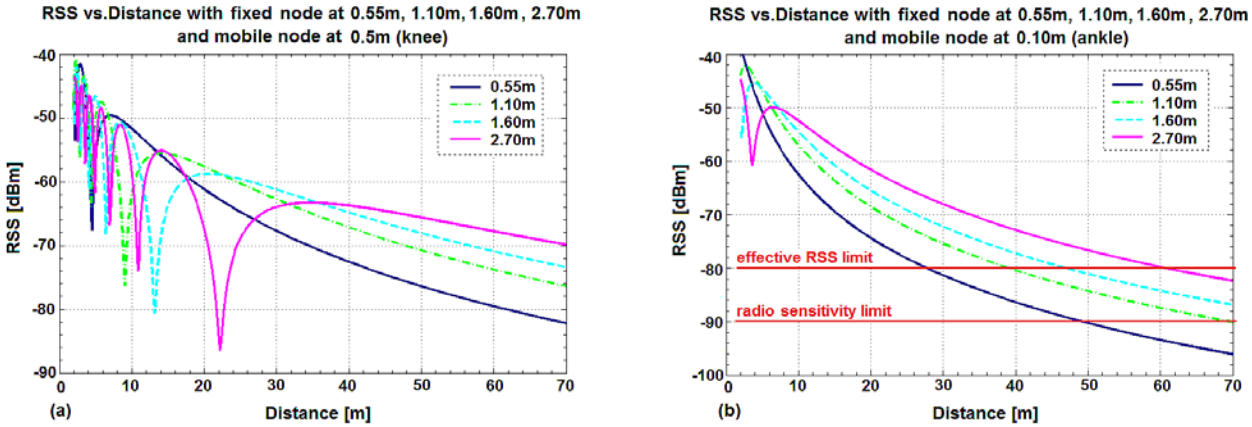

Figure 7. Behavior of the propagated signal or RSS concerning different heights for the fixed nodes and: a) knee and b) ankle mobile node position

Almost the same applies to the ankle case for which RF propagation results for the beacons' heights at 2.7m, 2.10m, 1.60m and 0.55m are shown in Fig. 7(b). The propagation curves are without 'null' regions and resemble the propagation of the widely used long-distance path loss model [13]. The beacons height at 0.55m seems the most suitable due to the most inclined curve slope. However, considering that the Tmote-Sky radio sensitivity level is about -90dBm,, then the communication between the mobile node and the beacons, when the distance is approximately 45m-50m, could be seriously limited or totally fail, which results in insufficient received packets for performing the tracking task. This implies that, for the ankle case, the fixed nodes should be placed at a height above 1.00m in order to maintain an "effective" RSS level at 50m assuring robust communication between the mobile node and the beacons.

As a conclusion of this analysis, the combinations of 0.55m mobile height with 0.55m beacon height, and 0.15m mobile height with beacon height above 1.00m present high potential for successful tracking.

C. *Analysis of the mobile node height variability due to movement*

From the analysis performed in the previous two sections, some of the mobile-node-height/beacon-height combinations are selected for further investigation for their approval like appropriate topology parameters. These combinations are:

- height of 0.55m for the mobile node and height of 0.55m for the beacon nodes, i.e., knee case,
- height of 0.15m for the mobile node and height above 1.00m for the beacon nodes, i.e., ankle case.

Another factor that may influence the behaviour of the propagated signal is the height variation of the mobile node due to the movement of the human body. Depending on the mobile node position, its height varies during the body movement as shown in Table I. This variance ranges from 10cm at the knee to 1 m at the wrist. Since the knee and ankle positions, were selected as the most promising positions, only the variation of these two positions will be analysed.

According to Table I the ankle movement varies between 0.15m and 0.30m during walking. In order to study the behaviour of the propagated signal due to the variation of the mobile node height, several simulations are performed. The height of the beacons is chosen at 1.50m, and for the mobile node three heights are selected: 0.10m, 0.20m and 0.30m. The simulated results for the three mobile heights are shown in Fig. 8(a). If we suppose that the ankle can change its height within 20cm during walking, then this corresponds to about 10dBm variation of the RSS measurements. If the RSS is measured during walking, this variation will be expressed like spikes up and down around the average propagation curve.

The average value for knee height is selected at 0.55m. During walking the knee height does not change more then ±5cm. However, there is another factor that imposes more variability of the knee height namely the difference among the people's body heights. Taller people have knee height approximately at 0.65m, while short people about 0.45m. Based on this, for the simulation about the influence of the knee height on the RF signal propagation we select four knee heights: 0.40m, 0.50, 0.60 and 0.7m. The selected values are a bit lower or higher that the real ones, so as to assure that we do not underestimate the knee-height variability effect over the RF propagation. Fig. 8(b) depicts the RF propagation results for the four knee heights when the fixed node is at 0.65m. The results show that the knee case is less influenced by the knee height variation, as a variation of 30cm causes the RSS-level to vary about 5 dBm. As in the ankle case, the height variation due to walking will be expressed like spikes up and down around the average propagation curve, which is discussed in Section V.

Considering the analysis in this section, obstacles are either absent or have an equal effect on all cases. In any other case, obstacles should be modeled appropriately.

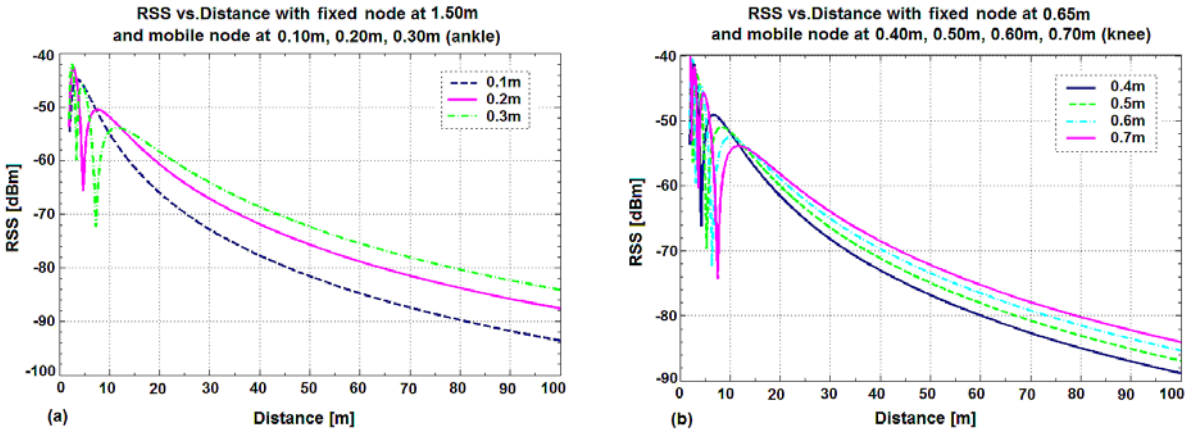

Figure 8. RSS behavior for different fixed node heights and: a) 0.1m or b) 0.5 m for the mobile node

IV. TARGET TRACKING CONSIDERATIONS AND SIMULATIONS

The analysis in Section II and in Section III clarified that knowing the RF propagation of the target environment and making careful selection of the heights and positions of the beacons and the mobile nodes, theoretically present possibility for performing RSS-based tracking with WSNs successfully.

In this section, the tracking technique, the factors influencing the tracking accuracy and the simulation procedure are discussed.

A. The Tracking Technique

As it was mentioned in Section II the fingerprinting approach is utilized in the present work. It is based on acquiring reference points within the target area (the triangle in our case). To these reference points are associated signature vectors consisting RSS data taken by each of the beacon nodes. The signature vector is formed by simulation performed with (1), i.e., FOM. All reference points positions and their signatures construct a database. During the localization phase, the RSS measurements, taken from the beacons for a particular mobile object, form a tested signature, which is compared with the signatures in the database to find the likeliest one and then the corresponding reference point location. Two techniques for defining the locations of the reference points are evaluated, namely quantized levels and square grid.

(a) Quantized Levels Approach

The quantized levels approach is based on dividing the RSS range between -40dBm and -90dBm in discrete levels, to which correspond different distance regions. The division is made so that each level can have almost the same width in dBm, and at the same time the width to be approximately 10dBm. In this sense, five RSS levels are chosen for the RF propagation curve when the fixed node height and the mobile node height are at 0.55m, as shown in Fig. 9(a). The corresponding distance ranges suppose tracking accuracy of 10m. It is observed that at short distances, up to 10m, the signal is a bit variable with small and narrow ‘nulls’, which

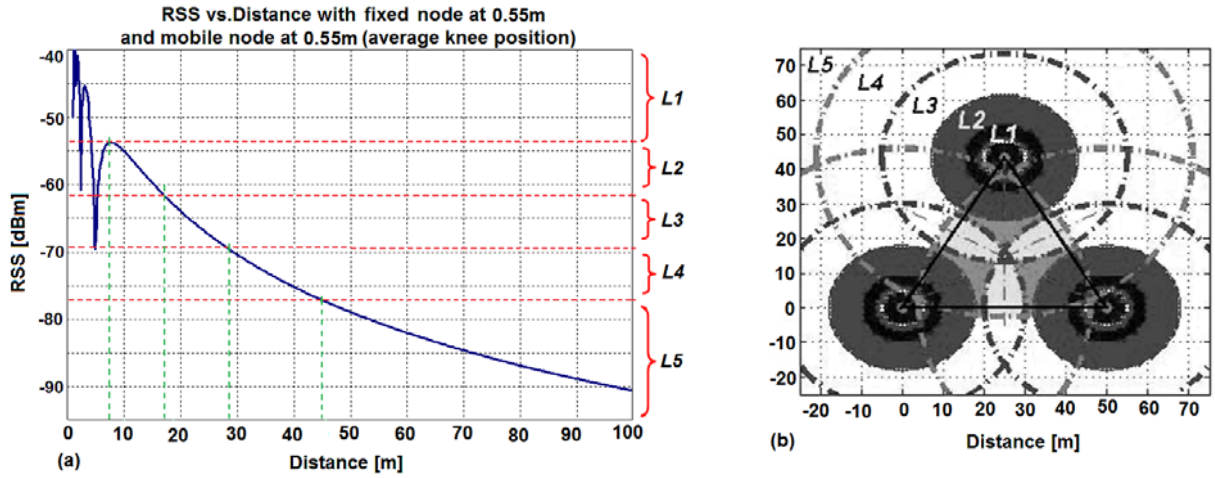

Figure 9. Quantized levels topology at 0.55 m (knee position) and fixed node at 0.55 m:
a) RSS vs. distance and RSS-levels, b) separation in recognizable RSS levels

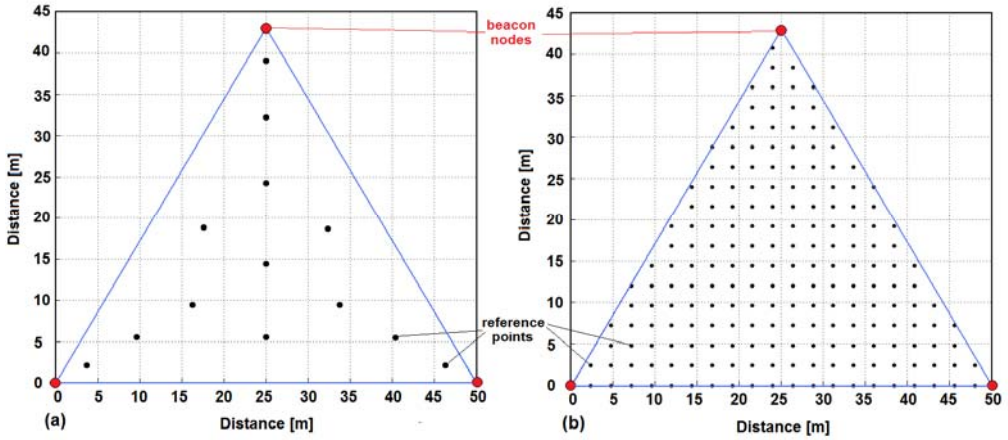

Figure 10. Reference points topologies for: (a) quantized levels techniques with 13 points, and (b) square grid technique with 289 points

may impose difficulty when estimating the mobile object position. Nevertheless, it can be filtered or handled by the use of an additional sensor such as ultrasound or passive infra-red (PIR) with respective techniques proposed [15].

The location of the reference points is chosen so that at least one reference point can exist in each region, differentiated by the discrete levels. An example of separation of the triangle area in recognizable RSS regions is shown in Fig. 9(b). According to this simulation 13 distinguishable regions are identified and hence 13 reference points are selected. The topology of the 13 reference points is shown in Fig. 10(a). The positions of the reference points have to be recalculated for each beacons-height/mobile-node-height combination.

The tracking task takes place inside the triangle when the RSS level provided by each of its fixed nodes is above level L5. If one of the fixed nodes receives RSS level 5, then the triangle may have to be changed and the tracking task to be transferred to the neighbourhood triangle. Concerning the interior of each triangle, there are some well-defined regions being characterized by different combination of each fixed node RSS. Using these regions, the position of the mobile node can be tracked with accuracy of about 10m at the centre of any of these regions.

(b) Square Grid Approach

The square grid approach for generation of the reference points is quite simple. The target area is divided out in small squares, the size of which determines the minimum localization accuracy. Such a reference-point grid is shown in Fig. 10(b). The size of the squares could be 1/10, 1/20, 1/25 and 1/50 of the beacons' distance to which correspond the following number of reference points: 81, 289, 441 and 1764.

During the tracking task, to every reference point is associated a vector-signature, consisting of the simulated RSS between the reference point and each beacon. The positions of all reference points as well as their signatures compose the signature database.

(c) Extension of the 50m Topology

The above analysis is based on the assumption that the distance among the beacon nodes in a triangle is 50m. Having selected the maximum transmission power of 0dBm, a combination of heights for both fixed and mobile nodes is required for guaranteeing fulfilment of the tracking task requirements. However, this particular analysis can also be held for other dimensions, since the combination of heights can be matched to the new required distances in order to produce similar RF signal propagation as for 50m. The same behavior can be achieved by increase of the beacons' height or by increase of the transmission power through connecting an external antenna with higher gain or through using another platform with greater transmission power. Fig. 11 shows simulations of the RF signal propagation, when the mobile node height is at 0.55m, i.e. knee. Three cases are presented: fixed node at 0.55m and 0dBm transmission power, fixed node at 0.55m and 4.5dBm transmission power, and fixed node at 1m and 0dBm transmission power.

The aim of these simulations is to investigate the situation where the communication distance between the beacons has to be increased, for instance to 70m, and thus how the topology parameters have to be modified in order

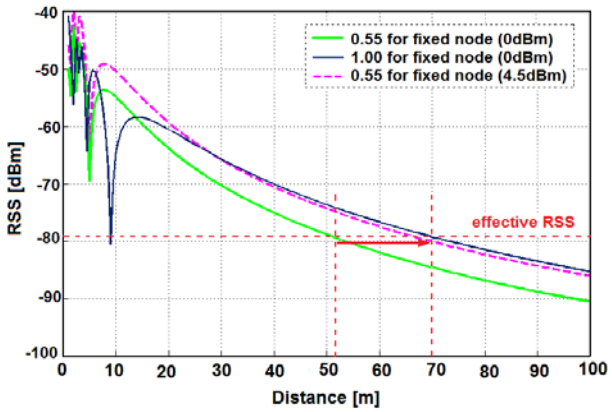

Figure 11. Extension of the 50m topology to a 70m topology

the new RF propagation to fit the one produced by the topology of 50m beacons' distance. The results from Fig. 11 show that it may not be necessary any parameters to be modified, since the RSS in 70m is around -85dBm, which is above the sensitivity threshold of the radio chipCC2420. Nevertheless, this value is lower than the adopted safe threshold level of -80dBm and according to [22] doubles the percentage of the packet loss. Therefore, it is advisable the RSS in the end distance of 70m to be around -80dBm, which require some parameter modifications.

The first and easier solution is to increase the beacons' height, since the mobile is fixed at the knee. As it is shown in Fig. 11, if the beacons' height is 1m, then the propagation curve shifts up and the RSS at 70m is around -80dBm. Unfortunately the last 'null' now is deeper and wider, and it is located at greater distance. In addition, the curve slop is not that inclined, which may worsen the tracking accuracy.

The second solution, which requires other sensor node platform, or more powerful antenna, is to increase the transmission power. As it is shown in Fig. 11 if the transmission power is 4.5dBm the propagation curve is exactly like the one for 0dBm, but up-shifted. This shift is enough so that the RSS at 70m to be -80dBm.

The two solutions have advantages and disadvantages. The first uses the same hardware, but may have less accuracy, while the second keep the same accuracy as for 50m distance but require hardware modification and will have more energy consumption.

B. *Other Factors Influencing the Tracking Accuaracy*

In the sections above we analysed the most important topological parameters to determine their importance and effects on the tracking task performance. However, knowing them is not enough for realistic tracking simulation or for contracting a reliable tracking algorithm. There are two factors that also have to be known and included during the simulation procedure or to be used for designing a tracking algorithm, and these are:

- The variability of the RSS due to its noisy nature and due the movement of the human body, and
- The sensor nodes' hardware variability, which may cause difference of 10dBm in the RSS measurements for the same parameters distance, height and transmission power.

(a) RSS uncertainty

As it is well known, RSS does not have a deterministic behavior, but presents random variation. This is most likely due to the radio hardware, nodes movement and incomplete description of the RF communication link. It is of great importance for the localization and tracking applications to identify and characterize the RSS uncertainty sources as well as to model them for more realistic tracking simulations [23]. In order to investigate the RSS variability when the transmitter and receiver are static, and when the transmitter is mobile and the receiver is static, several outdoor measurements were performed. Detailed description of the measuring setup and modelling procedure are given in [23].

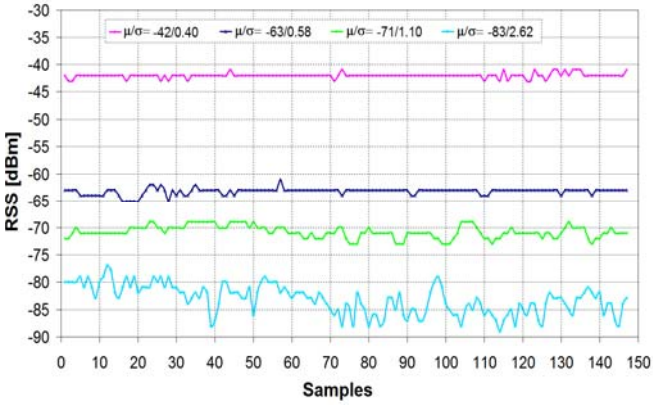

Figure 12. RSS measurements for four different combinations of μ and σ

The measurements for static transmitter and receiver were performed for different heights from the ground and distances in order to have more distinct RSS levels. Then the mean value μ and the standard deviation σ were calculated. Since the noise is considered to derive from multiple factors we assume Gaussian distribution. Fig. 12 presents RSS measurements for four different μ/σ combinations in dBm: -42/0.40; -63/0.58; -71/1.10 and -83/2.62. As Fig. 12 presents, the strongest signal, i.e., highest μ, has the smallest deviation, and the lowest signal has the highest deviation, i.e., the measured values are more dispersed regarding the mean value. It is noticeable that with the decrease of the signal strength the standard deviation increases, which could be expressed as $\sigma = f(\mu)$.

The measurements for fixed receiver and mobile transmitter were performed during human walking along a circle arc of 20m and 30m for the knee position case and of 15m and 25m for the ankle position case with speed of approximately 1m/s. The fixed node is in the centre of the circle arc and receives the transmitted signals of the mobile node positioned above the knee. In Fig. 13, we present the results for the RSS variation due to the movement of the

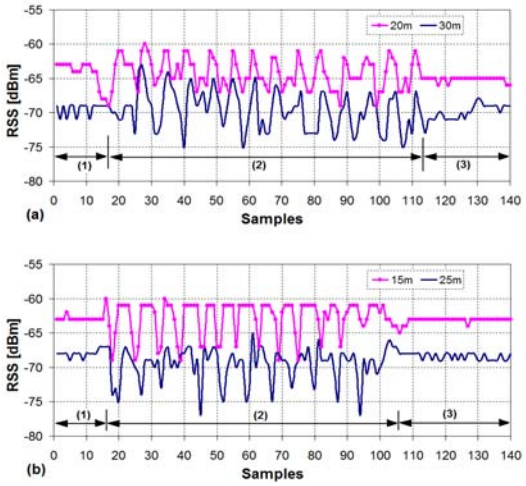

Figure 13. RSS measurements for (a) knee and (b) ankle transmitter position

transmitter, while the human walks. These plots have three distinguishable regions: (1) two seconds in immovable state, (2) walking state and (3) three to four seconds in immovable state. The average RSS value corresponds to the steady position of the human body, where the mobile node has stable height 0.55m from the ground. As it was expected, except for the RSS uncertainty owning to the RSS nature, there is an additional uncertainty introduced by the motion of the mobile node. The RSS variation due to the body movement is periodical and can be correlated with the trajectory of the legs movement. In particular, during walking, the height and antenna orientation change in a periodic manner, which results into periodic variations, i.e., spikes up and down around the mean value, of the RSS.

The modeling of the relation $\sigma = f(\mu)$ consists of data-to-curve-fitting approximation over the measured data [23]. The modeling equations for static transmitter, shown in Fig.12, and for mobile transmitter, shown in Fig. 13, are (3) and (4) respectively.

$$\sigma(\mu) = a.\exp(-b.\mu) + c\,, \tag{3}$$

where $a = 0.04$, b= -0.045, $c = 0.2$

$$\sigma(\mu) = a.\mu + b\,, \tag{4}$$

where a = -0.029 and $b = 0.48$.

Equation (3) is to be used in RSS uncertainty generation process depending on the mean value when the sensor nodes are fixed in outdoor unobstructed environment, while (4) includes both the uncertainty due to RSS nature and the uncertainty due to movement and it is to be used in noise generation process depending on the RSS mean value when the transmitting node is mobile.

(b) Sensor Node Hardware Variability

It is well known that there are differences in the radio circuits among the same type of transceivers. This hardware variability, due to production tolerance, leads to difference among actual transmission powers for the same sensor node types. To study the transmitter and the receiver variability several experiments were conducted [12]:

- one receiver and five different transmitters, and
- one transmitter and five different receivers.

The orientation and the position of the receivers and the transmitters are exactly the same. The height from the ground of the receivers and the transmitters is 0.70m. The experiments are performed for three different transmission powers of 0dBm, -3dBm and -11dBm at 50m, 30m and 15m T-R distances, respectively. The results are shown in Fig. 14.

The hardware variability of the transmitters and receivers results in difference of the measured RSS when five transmitters send and one receiver receive, as shown in Fig. 14 in the first column, and when one transmitter sends and five receivers receive, as shown in Fig. 14 in the second column. Moreover, the results present that the variation of the RSS among the five transmitters and receivers does not follow the same logic when change the transmission power. For instance, the node with ID 3, as a transmitter, has the highest RSS value for transmission power -3dBm at 30m in Fig. 14(c) and the lowest RSS value for transmission power -11dBm at 15m in Fig. 14(e). Similar observations hold for the results of the five receivers.

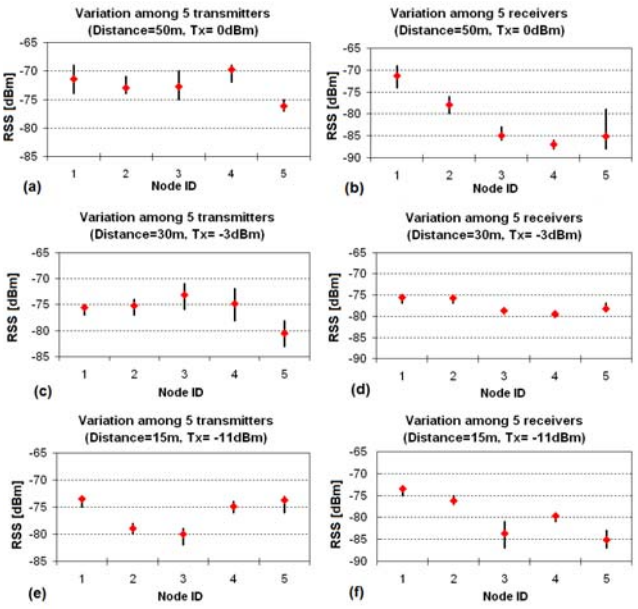

Figure. 14 Variation of the transceivers

Taking into account the results from Fig. 14, there is one more parameter to be included in (1), which represents the offset that the hardware imposes, and that is the P_{offset}. Thus, the received power can be expressed as:

$$\overline{P_R}(d) = P_T\left(\frac{\lambda}{4\pi d}\right)^2\left(K_1^2 + K_2^2\Gamma^2 + 2K_2\Gamma\cos\left(\frac{2\pi}{\lambda}\Delta L\right)\right)P_{offset} \tag{5}$$

where P_{offset} is given in mW in this equation and expresses the difference between the RSS produced by simulation with (1) and the real measured RSS. Therefore, the hardware variability strongly requires a calibration procedure before any tracking task.

C. Simulation procedure

The simulation process aims at simulating a target-tracking scenario considering all the topology parameters and factors that influence the tracking performance which have been discussed in the previous sections. As a location positioning technique the fingerprinting approach is utilized. It is based on acquiring reference points within the target area. The reference point topology is either constructed as a square grid with eligible square size, or is based on the points extracted by the quantized levels technique. Both of them were discussed in Section IV A and will be evaluated during the simulation procedure. Furthermore, in order to deal with the uncertainty of the propagated curve introduced by the first 10 meters, as shown in Section III, an additional sensor is assumed providing almost 10m range detection around a fixed node.

Part 1: Initialization of the input parameters

1. Load antenna model: (*InvertedF_model*)
2. Define input parameters: f (working frequency), c (velocity of light), λ (wave length), ε_r (relative permittivity of the ground), P_{TX} (transmission power)
3. Define model input parameters:
   (1) H_{ref} : Reference Height for RSS signature definition (knee or ankle)
   (2) H_r : Height for the fixed nodes (anchors)
   (3) H_t : Height for mobile node (knee or ankle)
   (4) H_{var} : Height variance due to movement
   (5) $Range_{sensor}$: Additional sensor range detection
4. Define area input parameters:
   (1) Distance X (e.g. *FieldX*=50m or 70m)
   (2) Distance Y (e.g. *FieldY*=50m or 70m)
   (3) Number of anchors (*AnchorsNumb*=3)
5. Calculate anchors coordinate:
   Anchor3Y= round (*FieldY**sqrt(3)/2);
   X_Anch=[0,*FieldX*,*FieldX*/2];
   Y_Anch=[0,0,*Anchor3Y*];
6. Define localization input parameters:
   Define number of grid points (*NumbGrPoints*)
   Define grid points coordinates

Calculation of the point's signature

7. for i=1:*NumbGrPoints*
8. for m=1:*AnchorsNumb*
9. Compute distance between anchors and the points: *AnchDist*
   (Compute RSS)
10. *RSS* = RSSmodel (H_r, H_{ref}, *AnchDist*, ε_r, P_{TX}, λ)
11. Save X, Y, *AnchDist*, *RSS* in {*GridPoints*}
12. *RSS_Signature* (i, m) = *RSS*;
13 end for
14. end for

Neural Network initialization & creation

15. [rows,columns] = size (*RSS_Signatures*);
16. *T* = [1: rows];
17. *net* = PNN (*RSS_Signatures*,T);

Generate mobile node path

18. Create mobile node's path, or load mobile node's path as *RealCoord* (X,Y)
19. Compute the number of the mobile positions, *NodesNumb*

Figure 15. Pseudo code for Part 1: Initialization

Part 2: Mobile node tracking

20. for i=1:*NodesNumb*
21. *Xn*=NodesCoord (i, 1);
22. *Yn*=NodesCoord (i, 2);
23. *HtVar*=*Ht*+sign* H_{var} *rand (1);
24. for m=1:*AnchorsNumb*
25. Compute Dist (*X_Anch*, *Y_Anch*, *Xn*, *Yn*)
26. if *Dist* < $Range_{sensor}$
27. CloserAnchorID = m; FlagCloserAnchor = 1
28. end if
    (Compute RSS)
29. *RSSnoNoise* = RSSmodel(*Hr*,*HtVar*, *Dist*,ε_r,P_{TX},λ);
    (Include noise to RSS)
30. *RSSmeasured* = noise(*RSSnoNoise*);
31. *MobileNodeRSS_signature* (1,m)= *RSSmeasured*;
32. end for
33. [*S*, *P*] = PNNsim(net, *MobileNodeRSS_signature*);
    (Filter signatures-probabilities if an anchor is close)
34. if *FlagCloserAnchor*==1 (An anchor is close)
35. [*S*, *P*] = Filter (S, P, *CloserAnchorID*);
36. end if
    (Acquire the maximum probability index)
37. *index* = maxProbability (*P*);
    (Obtain the coordinates of the estimated position)
38. *MobileNodeCoord* (i,1)=*GrPoints*(*index*,1);
39. *MobileNodeCoord* (i,2)=*GrPoints*(*index*,2);
40. end for
41 (Possible use of Filtering algorithm, such as Kalman filtering)
42. for i=1: *NodesNumb*
    (Compute absolute distance errors for each position)
43. ErrorDist (i) = (*MobileNodeCoord*, *RealCoord*);
44. end for
    (Compute RMSE)
45. *RMSE* = sqrt (mse (ErrorDist));

Figure 16. Pseudo code for Part 2: Tracking

In general, the simulation procedure is divided into two parts: (1) defining the needed functions, and initialization of the input parameters and the topology of the reference points named as virtual grid points; and (2) tracking of a mobile node on preliminary generated path. The pseudo code of the simulation procedure is given in Fig. 15 and Fig. 16 for its two parts respectively and is described briefly as follows.

Part 1: From step 1 to step 5 all needed parameters concerning the deployment are initialized, where reference height for RSS signature definition is the average height obtained by the corresponding to the knee or ankle movement presented in Table I. In Step 6, the coordinates for the virtual grid points are calculated. With steps 7 to 14, for all grid points, a signature consisting of three RSS measurements from the fixed anchor nodes is calculated and stored in {*RSS_Signature*}. Steps 15 to 17 initialize and create a probabilistic neural network (PNN) representing the search and matching algorithm used by the particular fingerprinting tracking scheme. PNN combines non-parametric probability density estimation with minimum risk decision making [20]. The density estimation implements the Parzen window estimator [19] by using a mixture of Gaussian basis functions.

After the estimation of the probability density functions for all signatures in {*RSS_Signature*}, the posterior probabilities are computed, and then the Bayes' optimal decision rule is applied to select the index of the winning signature. Finally, the last steps 18 and 19 create or load the mobile node path as *RealCoord*(*X,Y*) and calculate the mobile node movement positions. This part concluded the initialization of deployment parameters, functions and grid point attributes, forming the input to part 2.

Part 2: In steps 24 to 28, for each position of the mobile node track, the distance *Dist* with respect to each of the three beacon nodes is calculated. In the steps 29 and 30, this distance is used as a parameter in the RF propagation model, which generates the respective RSS including the uncertainty

due to movement variance calculated with (4). The variable height, *HtVar*, which the mobile node has in each position of the corresponding track, is calculated on the mobile node height H_t (ankle or knee) base within $\pm H_{var}$ deviation range because of the movement. In step 31, the RSS values from the three fixed nodes are stored as *MobileNodeRSS_signature* for further processing with PNN. The latter is used to discover the best matching signatures (vector *S*) from *RSS_Signatures* to the mobile node by computing their respective probability (vector *P*). In steps 34 to 36, depending on the presence of the mobile node in the detection range of the additional sensor attached to the fixed nodes, an appropriate filtering to the RSS signatures is applied selecting those corresponding to points close to a particular fixed node. Steps 37 to 39 gives the index ID of the signature with the highest probability and its corresponding coordinates, extracted from the *GrPoints* database, are coordinates for the mobile node. After the coordinates of the mobile node are identified it is possible of using filtering algorithm, such as Kalman filtering [24] in order to improve the tracking performance. Finally, the absolute distance error is computed for every mobile node position in the track as well as the root mean square error metric (RMSE) of the whole track.

D. Simulation results

The simulated area is an equilateral triangle with three fixed nodes on its vertices acquiring the RSS values of the received message from the position of the mobile node being tracked. The simulated path of the latter is comprised of points inside the triangle considering the fact that for real deployments if the mobile node inserts an adjacent triangle area, then the tracking task is undertaken by the respective fixed nodes. Moreover, for more realistic simulation over the simulated RSS, noise is added, calculated with (4), to represent the RSS variability due to human walking.

The main objective of the performed simulations is to obtain the tracking accuracy expressed by the RMSE metric in order to evaluate the selected topology parameters. The evaluation includes:

- the ankle and the knee positions' accuracy,
- the number and topology of the reference points,
- the filtering of the mobile node localization positions to perform tracking.

(a) Mobile Node Localization without Filtering

The first simulation performs localization of a mobile node located at 0.55m height in triangular area. For more realistic simulation over the simulated RSS, noise is added, calculated with (4), to represent the RSS variability due to human walking. The results from the simulation are presented in Fig. 17 for the two reference points' topology: square grid in Fig. 17(a) and quantized levels in Fig. 17(b). The located positions of the mobile node in these simulations are not filtered and it is difficult to estimate the simulated track. However, the average accuracy for both reference points' topologies is expressed as RMSE over the entire path and could be improved with any filtering algorithm. The RMSE is calculated over the entire mobile path for each point. The mobile path is calculated so as to represent walking with 1m/s. The results present that the localization accuracy is a bit better with the quantized levels reference point topology, than with the square grid topology. In this sense, the more the number of reference points increases, the less accuracy is obtained. Hence, we can conclude that without filtering algorithm the quantized levels reference point localization is better as a choice. To confirm this, more simulations are performed with square grid reference point topology for different points' number, presented in Table II. The results presented in Table II may vary within 5% from one simulation to another due to the randomness of the noise. However, the results show clearly that the number of reference points when the walking noise is included is minor factor for the accuracy of the localization process. But, if the computation time and computational resources are considered, then less points produce better performance.

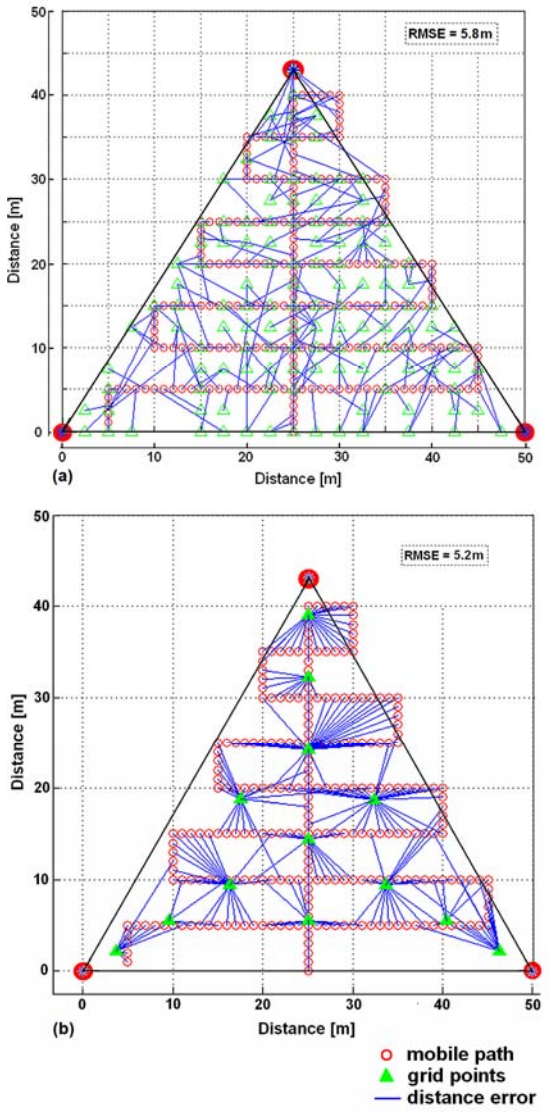

Figure 17. Tracking accuracy distribution for virtual grid density of: a) 289 points and b) 13 points

TABLE II. RMSE FOR DIFFERENT REFFERENCE POINTS NUMBER

Number of reference points	RMSE without filtering algorithm	RMSE with filtering algorithm
81	6m	2.8m
289	5.8m	2.7m
441	5.9m	2.6m
1764	6m	2.8m

(b) Mobile Node Tracking with Kalman Filtering

The second simulation repeats the first but with Kalman filtering [24, 25] performed on the localized mobile node positions, in order to complete the tracking task. The results are presented in Fig. 18 for the two reference point topologies.

The results present that the quantized-levels-reference-point topology, shown in Fig. 18(b) does not have resources for better tracking performance with Kalman filtering due to irregular location and small number of the reference points. Referring again the Table II, for reference point topology with squares' size smaller than 1/10 of the beacons' distance, i.e., more than 80 number of reference points, the tracking task can be completed through Kalman filtering with 50% improvement of the RMSE. Therefore, when tracking application is implemented through any filtering algorithm, the square reference point topology is preferable due to the uniform location and sufficient number of the reference points, unless more reference points are associated to the quantized levels topology.

(c) Ankle and Knee Positions' Accuracy

The input parameters for the last simulated scenarios are presented in Table III. The main goal is to study the localization accuracy, expressed as RMSE, depending on the mobile node positions, the beacon nodes height and the reference point topology.

According to Table III, the knee position is simulated for a 50m beacons' distance and for various fixed node heights. The signature of the reference points is calculated for the average knee position of 0.55m. However, during the simulation, the mobile node height varies from 0.45m to 0.65m, to represent the difference in the people's height. Ten simulations per each height are performed and the RMSE is averaged. The same reasoning implies also for the ankle case, the average height in which is considered as 0.20m and varies from 0.15m to 0.30m. The simulation results are presented in Fig. 19 and present the change in tracking accuracy, represented as average RMSE, for the two reference-points topologies. The average RMSE is produced by the localization procedure without Kalman filtering. The reference points are either 289 or 13 depending on the corresponding strategy used.

Fig. 19(a) and (b) present the situation when the mobile node is at knee position, i.e., 0.55m. The average RMSE is calculated for each of the allowed beacons' heights, discussed in Section II, when the heights of the mobile node

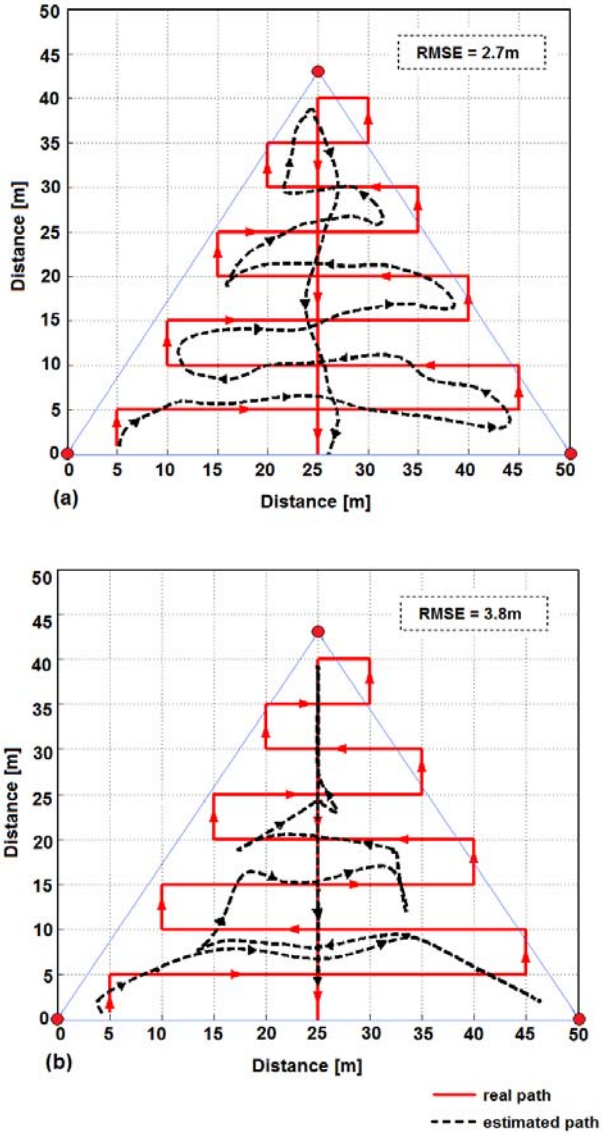

Figure 18. Tracking accuracy with Kalman filtering for reference point density of: a) 289 points and b) 13 points

TABLE III. INPUT PARAMETERS FOR THE SIMULATED SCHENARIOS

Scenario No	Mobile Node Reference Height	Fixed Node Height	Triangle Edge Size	Tx Power	Grid Points Number
1a	0.55m (knee)	0.55-1.60m	50 m	0 dBm	289
1b	0.55m (knee)	0.55-1.30m	50 m	0 dBm	13
2a	0.20m (ankle)	1.30-2.85m	50 m	0 dBm	289
2b	0.20m (ankle)	1.25-2.75m	50 m	0 dBm	13

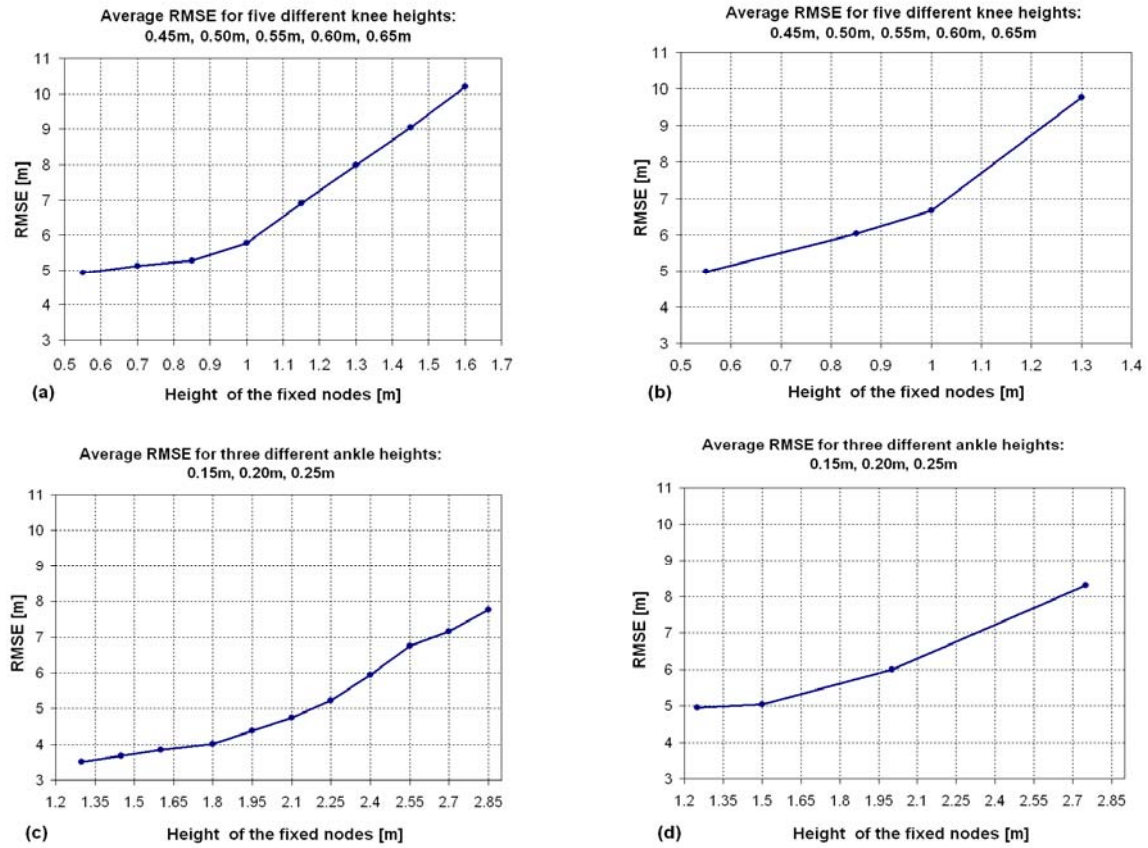

Figure 19. Tracking simulation RMSE distance based on different mobile node position on human body and number of RSS fingerprinting signature points: a) knee / 289, b) knee / 13, c) ankle / 289, and d) ankle / 13

change from 0.45m to 0.65m. Fig. 19(a) presents the square grid topology with 289 reference points, while Fig. 19(b) presents the quantized levels topology with 13 reference points. As it is shown, there is an increase in the loss of accuracy as the fixed node height increases. This observation stands for both the fingerprinting schemes of different reference point numbers having also similar accuracy values. As a conclusion, if the beacons' height is between 0.55m and 1m, then the localization accuracy is within about 6m for both the reference points' topologies.

In the second case, the ankle position is simulated in the same triangular area when the height variation of the mobile node ranges from 0.15m to 0.25m, while the beacons' node height ranges from 1.25m to 2.85m, according to the results from Section III B. The results are presented in Fig. 19(c) for square reference point topology and Fig. 19(d) for quantized levels topology. As in the knee case, the results for the two reference points' topologies present similarities. However, the case of the square grid topology with 289 reference points presents smaller RMSE than the case with the quantized levels topology with 13 reference points. Nevertheless, analyzing both topologies results, the obvious conclusion is that the RMSE is noticeably smaller when the beacons' height is in the range of 1.25m-1.65m.

V. PRACTICAL TRACKING EXPERIMENT

In this section, a real experiment is presented keeping the proposed topology parameters such as beacons' height and distance, and knee or ankle position for the mobile node, so as to perform a real outdoor tracking test.

A. Experimental Setup

From experiments performed for defining the variance of the RSS due to the body movement, we conclude that if the mobile node has not line-of-sight communication with beacon, for instance if it is attached to the inner side of a leg, the RSS drops about 20dBm compared to the value taken when the node is attached to the outer side of a leg. To overcome this problem, we attach one sensor node to each knee, as it is shown in Fig. 20. Thus, we take measurements from both mobile nodes and keep the strongest ones for the tracking task. The real results are much worse than the simulated ones. According to our understanding, this happens due to the offset that each node, mobile or beacon, imposes on the RSS measurements, and also due to rotation of the antenna, i.e., the mobile node and the non-equivalent antenna radiation in all directions.

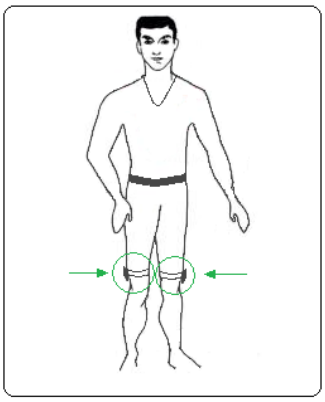

Figure 20. Positioning of two mobile nodes on the human body

The start-up requirements are:

- beacon nodes' distance of 45m,
- beacon nodes at 0.7m height,
- two mobile nodes (one at each knee) at 0.55m,
- walking with approximate speed of 1m/s,
- seven different measurements on the same walking trajectory,
- calibration measurements.

B. Measuring Process

During the tracking measurements a person with attached mobile nodes to his knees walks on preliminary drawn trajectory with speed of approximately 1m/s. The two mobile nodes send, one by one, a packet every second to the beacon nodes. The beacons send, within the time frame left of one second, their messages to the base station, including the RSS of the mobile nodes' packets.

After the tracking measurements, we perform also calibration measurements to evaluate the variability concerning the node hardware. The beacon nodes and the mobile nodes are located at 0.7m height and at distance of 20m. The two mobile nodes send 150 packets to the three beacons. From the measurements the average RSS value is calculated for each beacon. The difference between this value and the value produced through simulation with the propagation model (1) at 20m distance and 0.70m height gives the offset which can be included in (5). In addition, we compare the RSS measurements taken from each beacon during the walking with the RSS generated for the same node with the simulator (including the walking noise) to evaluate the offset. Finally, the results have shown that the beacons 1 and 3 have offset of about 5dBm regarding the ideal simulation and beacon 2 about 10dBm.

According to the specific results, an experimental system is not ready for real time filtering and tracking without dealing first with the calibration problems. Because of the hardware difference and the antenna radiation asymmetry the development of a generic calibration algorithm is extremely challenging. Therefore, the parameters for the calibration in the particular experiment have been calculated post-process.

C. Kalman Filtering

The next step is to apply Kalman filtering on the localized mobile coordinates in order to perform tracking. In order to use the standard Kalman filter to estimate a position, the process under consideration has to be able to be described by linear system equations. A linear system is a process that can be described by the following equations [25]:

$$x(k+1) = F\,x(k) + w(k), \quad (6)$$

$$y(k) = H\,x(k) + v(k), \quad (7)$$

Equation (6) is a state equation, while (7) is an output equation.

Here $x(k)$ is state vector and consists of the x, y positions and the corresponding velocities, $w(k)$ is the process noise with normal probability $p(w)\sim N(0,Q)$, $v(k)$ is the measurement noise with normal probability $p(v)\sim N(0,R)$, F is state transition matrix, H is observation matrix, Q is process noise covariance matrix and R measurement noise covariance matrix.

The implemented Kalman filter for the purpose of this work is based on the Kevin Murphy's toolbox [25]. The input parameters and the initialization of the needed matrices for the Kalman filter are shown in Fig. 21. A brief description of the code is as follows:

From Step1 to Step10 the state matrices are initialized. Step 13 and Step 14 calculate the process noise and measurement noise covariance matrices. Usually the process noise represented as *varianceQ* is small with values 0.1 or 0.01. The value *varianceR* represents the uncertainty in the measurement process and we accept that *varianceR* is 6 or 7, representing 6m/7m of measurement error. The matrices Q and R may change with each time step or measurement. Step 15 and 16 call the kalman_filter and kalman_smoother functions, which are from the Kevin Murphy's toolbox, and return the filtered coordinates as *xfilt*, *Vfilt* and *xsmooth*, *Vsmooth,* respectively. The new coordinates are saved in *Kalman_localized* and *Kalman_smooth* matrices during the Step 17 to Step 20. Step 21 plots the result and from Step 22 to Step 32 the RMSE of the results for pure localization, the filtering and the smoother are calculated.

D. Tracking Results

As it was mentioned above, seven different measurements on the same walking trajectory have been performed. The calibration of the beacons are fulfilled through comparison of the RSS measurements taken from each beacon during the walking (only for one measurement) with the RSS generated for the same node with the simulator (including the walking noise) to extract the offset for each beacon.

The tracking test has been performed for the two reference point topologies with the same input measurements and calibration values. For the square grid topology, 289 points are generated. For the quantized levels, this time, more regions are identified and consequently the number of the reference points is 19, instead of 13 in the simulation example. The calculated RMSEs for all seven measurements,

Kalman filtering

(input matrixes: *NodesCoord_real* and *NodesCoord_localized*)

```
1. X0=10;              % X beginning coordinate
2. Y0=0;               % Y beginning coordinate
3. Vx0=0;              %
4. Vy0=1;              %
5. ss = 4;             % state size
6. os = 2;             % observation size
7. x = zeros (ss, T);  % T -number of the measurements
8. y = zeros (os, T);
9. initx = [X0 Y0 Vx0 Vy0]';
10. initV = 1*eye (ss);
11. F = [1 0 1 0; 0 1 0 1; 0 0 1 0; 0 0 0 1];
12. H = [1 0 0 0; 0 1 0 0];
13. Q = varianceQ *eye (ss);     % Process noise covariance
14. R = (varianceR)^2*eye(os); % measurement noise covariance
15. [xfilt, Vfilt, VVfilt, loglik] =
                  =kalman_filter(y, F, H, Q, R, initx, initV);
16. [xsmooth, Vsmooth] =
                  =kalman_smoother(y, F, H, Q, R, initx, initV);
17. Kalman_localized(:,1)= xfilt(1,:)';
18. Kalman_localized(:,2)= xfilt(2,:)';
19. Kalman_smooth(:,1)= xsmooth(1,:)';
20. Kalman_smooth(:,2)= xsmooth(2,:)';
21. plot(Kalman_smooth(:,1), Kalman_smooth(:,2),'ks');
22. yR=[NodesCoord_real(:,1), NodesCoord_real(:,2)]';
23. y=[NodesCoord_localized(:,1), NodesCoord_localized(:,2)]';
24. allsr=length(NodesCoord_localized(:,1));
25. alls=length(Kalman_localized(:,1));
26. dReal = yR([1 2],:) - y([1 2],:);
27. rmse_real = sqrt(sum(sum(dReal.^2))/allsr);
28. dfilt = yR([1 2],:) - xfilt([1 2],:);
29. rmse_filt = sqrt(sum(sum(dfilt.^2))/alls)
30. dsmooth = yR([1 2],:) - xsmooth([1 2],:);
31. rmse_smooth = sqrt(sum(sum(dsmooth.^2))/alls)
```

Figure 21. Tracking with Kalman filter

for the two reference points' topologies are presented in Table IV. Two columns for each topology case are given to illustrate the difference in the RMSE when only localization of the node is required and when the tracking with filtering is implemented. As it is obvious, the filtering improves the accuracy. Another observation is that the quantized levels topology presents a bit better results most likely due to the careful selection of the position of the reference points. Visually there is no big difference between the tracked path from the one or the other reference point topologies, as it is shown in Fig. 22. Fig. 22(a) presents the real path and the tracked path from measurement 4 with square grid topology, while Fig. 22(b) presents the real path and the tracked path from measurement 2 with quantized levels topology.

The RMSE of all seven measurements, for the two reference point's topologies, presents relatively stable tracking accuracy, which is within the application requirements of 10m. However, without proper topology parameter selection and proper calibration procedure, the RSS-based tracking is impossible.

TABLE IV. RMSE FOR SEVEN MEASUREMENS

Number	RMSE Square grid, 289 points		RMSE Quantized levels, 19 points	
	Localization	Filtering	Localization	Filtering
1	13.2m	10.8m	11.8m	10m
2	13m	9.5m	10.3m	8.2m
3	12.3m	9.2m	10.9m	8.5m
4	10.8m	8.8m	9.4m	7.6m
5	11.2m	7.6m	9.3m	7m
6	12.3m	9.7m	11.3m	9m
7	12m	10m	10.8m	8.9m

VI. DISCUSSION AND CONCLUSIONS

The present study investigates the possibility a target tracking task to be performed with the resources of the WSN technology, when using only the RSS of the exchanged messages. In order to evaluate such a possibility the present study was focused on identifying the most crucial RSS-based tracking problems and to determine and evaluate the topology parameters that can guarantee successful tracking. More specifically we aimed at: (1) evaluation of the behaviour of the propagated RF signal in order to identify the important RSS-based tracking problems, (2) selection of the topology related parameters, when taking into consideration the tracking task requirements and the deployment constraints, (3) use of the selected propagation model and topology parameters to simulate a target tracking task, and (4) use of the proposed topology parameters to perform real outdoor tracking test. Hence, summarizing the obtained results the following conclusions were derived:

- During the modelling of the RF signal propagation several factors have to be considered, such as the height from the ground of the transmitter and the receiver, the frequency of the transmitted signal, the type of the ground (e.g. grass, road, etc.), the sensor nodes' hardware variability, the difference of the antenna gain for each of the supported frequency bands, the antenna pattern irregularities, and the RSS uncertainty.
- The RF signal propagation has to be considered when choosing the topology parameters, such as beacons' distance and height, in order to assure reliable communication between the beacons. The combination between the fixed node's height and distance is constrained by the fact that the communication among them has to be as robust as possible with respect to minimum packet loss. Therefore, the selected heights of the fixed nodes for reliable communication among them at distance, for instance of 50m are: 0.55m–1.60m; 1.85m–2.35m; and 2.55m–2.90m.
- The position of the mobile node on the human body should be selected so as to minimize the possibility for great node's height variation due to body movement in order to minimize the variability on the RSS due to this movement.

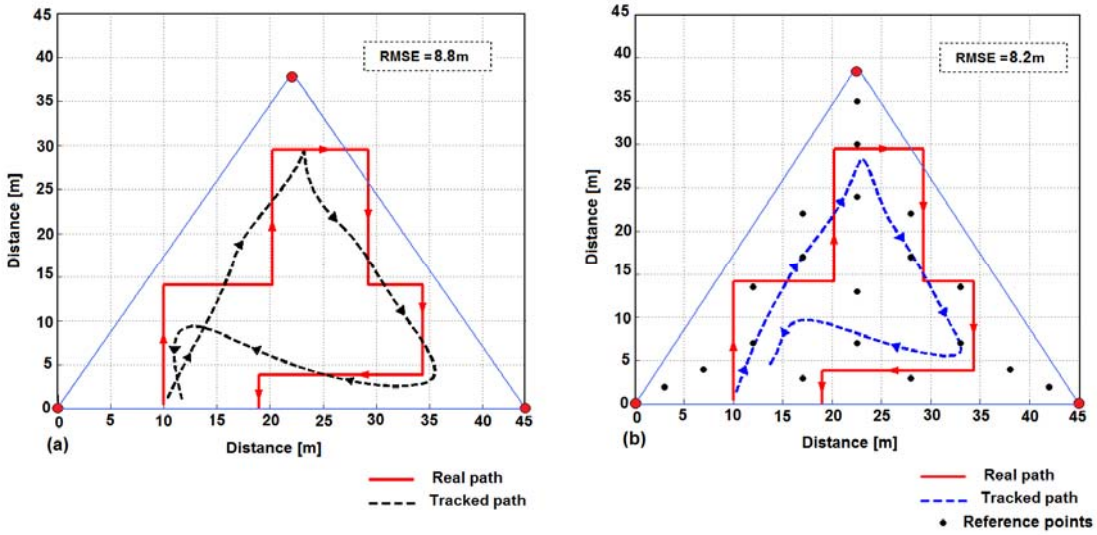

Figure 22. Tracking of a mobile node with Kalman filtering for:
(a) square-grid reference point topology with 289 points and (b) quantized-levels reference point topology with 19 points

- The RF propagation between the beacons and the mobile node has to be as smooth as possible to ensure that it has as few as possible 'nulls'. This can be achieved by judicious selection of the heights at both beacons and mobile node.
- When using the fingerprinting approach, the selection of the reference points' locations and topology needs preliminary evaluation according to well defined criteria such as the number of points, which define the computational load and the granularity of the localization accuracy as well, the required tracking accuracy, and finally, the simplicity of points generation, where the square grid is easier to be generated, while the quantized levels approach needs multiple calculations for each case of beacon - mobile node pair of heights.
- The hardware variability strongly requires calibration procedure before any tracking task. Because of this, the antenna radiation asymmetry and the possibility of unpredictable and continuous rotation of the mobile node, the development of generic calibration algorithm is extremely challenging. Without proper calibration procedure the RSS-based tracking is impossible.
- The filtering, such as the Kalman filtering, applied on the localized mobile node coordinates is absolutely essential for performing tracking, but it is not necessary when only localization is performed.
- The real outdoor tracking test demonstrates that the RSS can be used for outdoor localization and tracking applications under well-defined topology constraints and only after the proper calibration.

ACKNOWLEDGEMENT

The work reported here was performed as part of the uSWN FP6-2005 IST-034642 research Program and funded by the European Social Fund (ESF).

REFERENCES

[1] F. Kerasiotis, Ts. Stoyanova, A. Prayati, G. Papadopoulos, "A Topology-Oriented Solution Providing Accuracy for Outdoors RSS-Based Tracking in WSNs", Second International Conference on Sensor Technologies and Applications, SENSORCOMM 2008, August 2008, Cap Esterel, France, pp. 239–245 doi: 10.1109/SENSORCOMM.2008.122

[2] M. Cardei, J. Wu, "Energy-efficient coverage problems in wireless ad-hoc sensor networks", Computer Communications 29, pp. 413–420, Elsevier B.V, doi:10.1016/j.comcom.2004.12.025 2006.

[3] A. Savvides, C. Han, M. B. Srivastava. "Dynamic fine-grained localization in ad-hoc networks of sensors", 7th annual international conference on MobiCom 2001, Rome, Italy, 2001, pp. 166–179, doi: 10.1145/381677.381693

[4] D. Niculescu, B. Nath, "DV Based Positioning in Ad hoc Networks", Journal of Telecommunication Systems, Springer, Vol.22, Numb.1-4, January, 2003, pp. 267-280, doi: 10.1023/A:1023403323460.

[5] M. L. Sichitiu, V. Ramadurai, P. Peddabachagari, "Simple algorithm for outdoor localization of wireless sensor networks with inaccurate range measurements", International Conference on Wireless Networks, 2003, pp. 300-305.

[6] T. He, C. Huang, B.M. Blum, J.A. Stankovic, T. Abdelzaher, "Range-free localization schemes for large scale sensor networks", 9th annual international conference on MobiCom 2003, San Diego, CA, USA 2003, pp. 81–95, doi: 10.1145/938985.938995.

[7] F. Reichenbach, J. Blumenthal, D. Timmermann, "Improved Precision of Coarse Grained Localization in Wireless Sensor Networks" 9th Conference on DSD 2006, , Dubrovnik, Croatia, 2006 pp. 630-637, doi: 10.1109/DSD.2006.61.

[8] Hu, L., Evans, D., "Localization for mobile sensor networks", 10th Annual International Conference MOBICOM 2004, ACM, Philadelphia, US, 2004, pp. 45 - 57, doi: 10.1145/1023720.1023726.

[9] Y.-C. Tseng, S.-P. Kuo, H.-W. Lee, and C.-F. Huang. “Location tracking in a wireless sensor network by mobile agents and its data fusion strategies”, 2nd International Conference on Information Processing in Sensor Networks, IPSN 2003, Palo Alto, CA, USA, 2003, pp. 625–641.

[10] K. Mechitov, S. Sundresh, Y. Kwon, “Cooperative Tracking with Binary-Detection Sensor Networks”, 1st International Conference on Embedded Networked Sensor Systems, SenSys 2003, Los Angeles, California, USA, November 5-7, 2003, pp. 332-333.

[11] H. Yang, B. Sikdar, “A Protocol for Tracking Mobile Targets using Sensor Networks”, Proceedings of IEEE Workshop on Sensor Network Protocols and Applications, WSNA 2003, Anchogare, AK 2003.

[12] Ts. Stoyanova, F. Kerasiotis, A. Prayati, G. Papadopoulos, “Evaluation of Impact Factors on RSS Accuracy for Localization and Tracking Applications in Sensor Networks”, Special issue of Telecommunications Systems Journal, Springer, Vol.42, pp. 235-248, Dec. 2009, DOI: 10.1007/s11235-009-9183-8)

[13] T. S. Rappaport, Wireless Communications: Principles and Practice, 2nd Edition. Prentice Hall, 2001

[14] Ultra low power IEEE 802.15.4 compliant wireless sensor module, TmoteSky datasheet, Moteiv Co., 2006

[15] A. Smith, H.Balakrishman, M. Goraczko, N. Priyanha, “Tracking moving devices with cricket location system”, In Proc. 2th ACM MobiSys, Boston, MA, 2004, pp. 190-202, doi: 10.1145/990064.990088

[16] C. Alippi, G. Vanini, “A RSSI-based and calibrated centralized localization technique for Wireless Sensor Networks”, In Proc. 4th annual IEEE International Conference on Pervasive Computing and Communication Workshops 2006, PERCOMW’06, pp.301-305, doi: 10.1109/PERCOMW.2006.13

[17] Jian Ma, Quanbin Chen, Dian Zhang, Lionel M. Ni, "An empirical study of radio signal strength in sensor networks in using MICA2 nodes," HKUST, Technical Report, 2006

[18] Ts. Stoyanova, F. Kerasiotis, A. Prayati, G. Papadopoulos, “A Practical RF Propagation Model for Wireless Network Sensors”, In Proceedings of the 3d International Conference on Sensor Technologies and Applications, SENSORCOMM 2009, June 2009, Athens, Greece , doi: 10.1109/SENSORCOMM.2009.39

[19] E. Parzen, “On estimation of a probability density function and mode.”, Annals in Mathematical Statistics, 33:1065-1076, 1962

[20] D. F. Specht, “Probabilistic neural networks.” , Neural Networks, 3(1), pp:109-118, 1990

[21] “TelosB mote platform”, Crossbow Technology. Copyright 2009, http://www.xbow.com/Products/Product_pdf_files/Wireless_pdf/TelosB_Datasheet.pdf

[22] Ts.Stoyanova, F. Kerasiotis, A. Prayati, G. Papadopoulos, “Communication-aware deployment for Wireless Sensor Networks”, SENSORCOMM 2008, August 2008 - Cap Esterel, France.

[23] Ts.Stoyanova, F. Kerasiotis, K. Efstathiou, G. Papadopoulos, “Modeling of the RSS Uncertainty for RSS-based Outdoor Localization and Tracking Applications in Wireless Sensor Networks” SENSORCOMM2010, July 2010, Vinecia, Italy, (accepted for publication).

[24] Welch, Bishop, “An Introduction to the Kalman Filter”, UNC-Chapel Hill, TR 95-041, July 24, 2006, available from: http://www.cs.unc.edu/~welch/kalman/

[25] K. Murphy, “Kalman filter toolbox for Matlab” 1998 , available from: http://www.cs.ubc.ca/~murphyk/Software/Kalman/kalman.html